LBL-30417
Preprint

Lawrence Berkeley Laboratory
UNIVERSITY OF CALIFORNIA

Accelerator & Fusion Research Division

Submitted to Journal of Applied Physics

Modelling of H^- Surface Conversion Sources; Binary (H-Ba) and Ternary (H-Cs/W) Converter Arrangements

C.F.A. van Os, W.B. Kunkel, C. Leguijt, and J. Los

March 1991

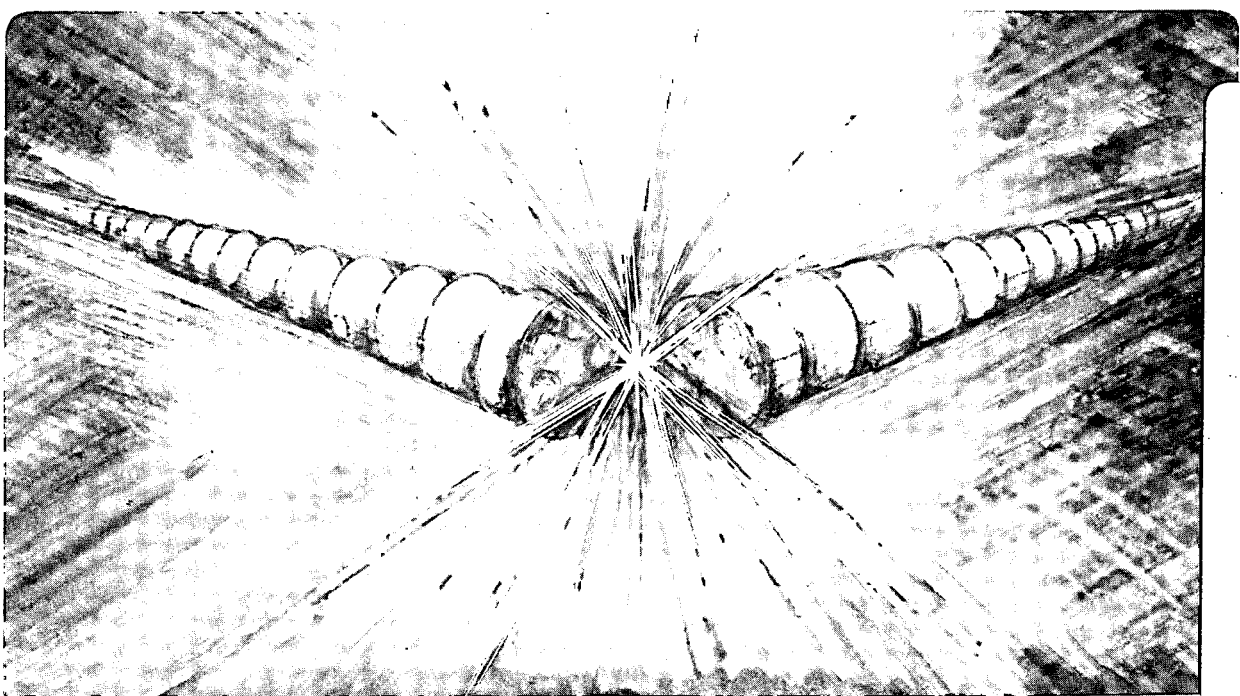

LOAN COPY
Circulates
for 4 weeks
Bldg. 50 Library.
LBL-30417
Copy 2

Prepared for the U.S. Department of Energy under Contract Number DE-AC03-76SF00098

DISCLAIMER

This document was prepared as an account of work sponsored by the United States Government. Neither the United States Government nor any agency thereof, nor The Regents of the University of California, nor any of their employees, makes any warranty, express or implied, or assumes any legal liability or responsibility for the accuracy, completeness, or usefulness of any information, apparatus, product, or process disclosed, or represents that its use would not infringe privately owned rights. Reference herein to any specific commercial product, process, or service by its trade name, trademark, manufacturer, or otherwise, does not necessarily constitute or imply its endorsement, recommendation, or favoring by the United States Government or any agency thereof, or The Regents of the University of California. The views and opinions of authors expressed herein do not necessarily state or reflect those of the United States Government or any agency thereof or The Regents of the University of California and shall not be used for advertising or product endorsement purposes.

Lawrence Berkeley Laboratory is an equal opportunity employer.

DISCLAIMER

This document was prepared as an account of work sponsored by the United States Government. While this document is believed to contain correct information, neither the United States Government nor any agency thereof, nor the Regents of the University of California, nor any of their employees, makes any warranty, express or implied, or assumes any legal responsibility for the accuracy, completeness, or usefulness of any information, apparatus, product, or process disclosed, or represents that its use would not infringe privately owned rights. Reference herein to any specific commercial product, process, or service by its trade name, trademark, manufacturer, or otherwise, does not necessarily constitute or imply its endorsement, recommendation, or favoring by the United States Government or any agency thereof, or the Regents of the University of California. The views and opinions of authors expressed herein do not necessarily state or reflect those of the United States Government or any agency thereof or the Regents of the University of California.

LBL-30417

Modelling of H^- surface conversion sources; binary (H-Ba) and ternary (H-Cs/W) converter arrangements.*

C.F.A. van Os and W.B. Kunkel

Lawrence Berkeley Laboratory, University of California,

1 Cyclotron Road, Berkeley, CA 94720, USA

C. Leguijt and J.Los.

Association EURATOM-FOM, FOM-Institute for Atomic and Molecular Physics,

Kruislaan 407, NL-1098 SJ AMSTERDAM, THE NETHERLANDS

ABSTRACT

The production process for the formation of H^- ions in a surface conversion source is sputtering of hydrogen atoms from the converter surface layers by incident positive ions, followed by electron attachment via resonant charge exchange with the converter surface. The sputtering process is in direct relation to the converter surface composition. New experimental data led us to indentify two different classes of converters: metallic converters, like solid barium (*binary*) and adlayer converters, like cesium on tungsten (*ternary*). For a binary converter the hydrogen in the surface layers is directly sputtered by the incoming ions. Consequently, the negative ion yield scales with the hydrogen concentration in the surface layers. In the cesium/tungsten system (ternary) the hydrogen at the surface is sandwiched between the cesium adlayer and the tungsten surface. Hence, the negative ion yield scales with the sputter coefficient of hydrogen on adsorbed cesium. This is experimentally confirmed.

* This work was made possible by financial support from the Nederlandse Organisatie voor Wetenschappelijk Onderzoek (NWO) and EURATOM and has also been supported, in part, by the Director, Office of Energy Research, Office of Fusion Energy of the U.S. Department of Energy under Contract No. DE-AC03-76SF00098.

I. INTRODUCTION

Neutral Beam Injection (NBI) in future TOKAMAK experiments[1] require the development of negative-ion sources. Two schemes to produce negative ions are under development: volume production and surface conversion. The first method is based on the extraction of H^- or D^- ions formed in the bulk of a plasma (e.g. by dissociative attachment of electrons to vibrationally excited molecules). In the second method, the negative ions are produced via electron attachment while interacting with a negatively-biased, low work-function electrode (converter) immersed in a hydrogen or deuterium discharge. In this paper, we present a study on the negative ion production process in surface conversion sources. We focus on the effect of the type of converter on the processes resulting in negative ions. Two types of converters are compared; a metallic converter (barium) and an adlayer converter (cesium on tungsten).

One of the first surface conversion experiments was done by Belchenko et al., who extracted a beam of negative hydrogen ions from a magnetron source.[2] These ions were produced at the cathode surface. It was generally believed that the conversion process could be better controlled if it was separated from the plasma production process. Therefore, in most subsequent experiments the negative ions are produced at a special isolated electrode, the so-called converter.[3,4,5,6] The converter should have a small work function to obtain a high negative ion yield.[7]

In a typical negative-ion source, the converter is biased at a negative potential V_c of a few hundred Volts, so that it draws a flux of positive hydrogen ions from the plasma sheath. A fraction of these ions is scattered. Furthermore, adsorbed hydrogen atoms are sputtered from the converter surface by incident positive plasma particles. The scattered and sputtered hydrogen particles can be ionized via charge exchange with the metal surface. Negative ions thus formed are accelerated across the plasma sheath, and can be aimed at an aperture through which they exit from the plasma, a process known as "self-extraction".[8] The ionization

process is operative over a distance of a few times the Bohr radius a_o, which is small with respect to the sheath thickness. The latter is typically a few μm in an intense discharge. Therefore, the charge exchange process between metal surface and hydrogen atom is not affected by the sheath potential.

By now, it has been well established that the negative ion beam produced from a surface conversion source, is mainly composed of negative ions formed via electron attachment to sputtered or recoiled atoms from the surface. This implies that the particle energy close to the surface is small compared with the sheath potential. Therefore, the energy distribution of the negative ion beam peaks around $e|V_c|$ electronvolt, where V_c represents the converter voltage.[9] Recent calculations of Belchenko and Kupriyanov confirm this observation.[10] The abundance of sputtered particles in the extracted beam is related to the applied geometry of the source.[11] The exit aperture is usually placed in a plane parallel to the converter surface, therefore only those particles emitted under more or less normal angles to the surface are able to leave the source.

In a geometry as described above, the production of a large flux of sputtered atoms is important to obtain a high negative ion yield. This paper will focus on the production of this sputtered flux for two different systems: i) a metallic barium converter where the formation process is the interaction of hydrogen with barium, *a binary system (H-Ba)* and, (ii) a cesiated tungsten converter where the interaction is between hydrogen and the cesium/tungsten surface, *a ternary system (H-Cs-W).* The most common cesiated-tungsten converter which has been employed is produced by admitting cesium vapor into the discharge chamber.[12] We will present model calculations which indicate that the dynamic cesium coverage obtained in this way is a strong function of the operational parameters, especially the converter voltage. Since the cesium coverage dramatically affects the work function of the converter, this system is not suited for comparison with an arrangement where the work function is constant (barium). Hence, experiments have been carried out in an arrangement where the cesium coverage is

obtained via surface wetting, a technique resulting in a full monolayer coverage of the tungsten surface, independent of the plasma characteristics and converter bias. This stable converter composition enabled us to model the hydrogen sputtering process in a way similar to the modelling done for a pure barium metal converter, and enabled us to compare both systems.

II. THEORY

The negative ion current density at the surface, J_{H^-}, can in its most general form be described as an integration over the parallel, v_p, and normal velocity, v_n, of an attachment probability multiplied by the flux of hydrogen atoms leaving the surface and an attenuation factor;

$$J_{H^-} = e \int_0^\infty dv_n \int_0^\infty dv_p \, \eta_H(v_n,v_p) \, \Phi_H(v_n,v_p) \exp\left(- \int_0^L dl \sum_i n_i \, \sigma_i(v_n,v_p)\right) \qquad [1]$$

where $\eta_H(v_n,v_p)$ denotes the attachment probability, $\Phi_H(v_n,v_p)$ denotes the flux of hydrogen atoms with a velocity between v and v+dv leaving the surface and the exponential function is an attenuation factor which describes the stripping of negative ions on molecules and plasma particles with their respective densities, n_i, and cross sections, $\sigma_i(v_n,v_p)$.

In a practical surface conversion source, only negative ions leaving more or less normal to the surface are collected. $\Phi_H(v_n,v_p)$ is a sum of particles which are reflected from the surface and particles which are sputtered or recoiled.[13,14] In view of the difference in angular distribution of sputtered and reflected particles, $\Phi_H(v_n,v_p)$ can be simplified by the assumption that only sputtered or recoiled hydrogen atoms contribute.

If the pressure in the surface conversion source is of the order of a few mTorr and the plasma density is below 10^{12} cm^{-3} then the attenuation term can be neglected if the path length, L, the negative ions travel is below 10 cm.[15,16] Since the energy with which the atoms are sputtered from the surface is small compared to the energy obtained by acceleration over

the sheath potential, we can formally integrate over v_p. Additionally, we can simplify our integration by taking an average energy with which the hydrogen atoms leave the surface. Eq. [1] then reduces to

$$J_{H_n^-} = \int_0^\infty dv_n\, \eta_H(v_n)\, \Phi_H^*(v_n) = \int_0^{eV_c} dE\ \eta_H(E)\, \Phi_H^*(E) \approx \eta_H(\langle E\rangle)\, \Phi_H^* \qquad [2]$$

where V_c denotes the converter potential, $\langle E\rangle$ the average energy of the sputtered particles and Φ_H^* the sputtered flux. In the following two sections we will discuss the two remaining factors, namely the ionization probability and the sputtered flux.

II.a Attachment probability

The process of forming a negative ion via interaction with a low work function surface is generally known as resonant charge exchange[17]. For a hydrogen atom scattered from a low work-function metal-surface, the probability for negative ionization (attachment) can be calculated using a stationary phase approximation[18,19]

$$\eta_H(E_s) = \eta_H'(v_n) = \frac{1}{v_n} \int_{z_0}^{\infty} N^-(z)\, \omega(z)\, \exp\left(\frac{-1}{v_n} \int_z^\infty \omega(z')\, dz'\right) dz. \qquad [3]$$

Here, $\omega(z)$ represents the transition frequency, $N^-(z)$ is the 'stationary' charge state at distance z, and z the distance between surface and atom. With this expression, the attachment probability can be calculated as a function of the energy of the hydrogen atom leaving normal to the surface. Using the experimental data from scattering experiments, under grazing angles of incidence, of van Wunnik et al.[20] and of van Amersfoort et al.[21] we can calculate the attachment probability. The result of this calculation is shown in Fig. 1 together with curves

obtained in a similar way for a tungsten surface covered with only half a monolayer of cesium and for a pure barium surface.

II.b Sputtered flux

In this section we will elaborate on the flux of sputtered and recoiled particles, which we will refer to as the sputtered flux. Generally, this flux is equal to an incident flux multiplied by a sputter coefficient. However, in this case we are interested in the sputtered flux of hydrogen particles from a surface. So in this case a description with a "solid body" sputter coefficient is inappropriate. Van Os, van Amersfoort and Los reported the use of a solid body sputter coefficient multiplied by the probability of hitting a hydrogen atom located at the surface.[13] This probability is related to the relative hydrogen concentration at the surface,

$$\Phi_H{}^* = \frac{c_H}{c_{sat}} \Gamma_{H\text{-}H} \Phi_H{}^+ \qquad [4]$$

where c_H denotes the hydrogen concentration at the surface, c_{sat} is the hydrogen saturation coverage, $\Gamma_{H\text{-}H}$ is the sputter coefficient for hydrogen on hydrogen and $\Phi_H{}^+$ is the incident flux of positive hydrogen ions. The concentration of hydrogen at the surface is due to implantation of the energetic hydrogen ions. This incident flux also erodes the tungsten surface which gives the surface an inward velocity,

$$v_{sput} = \frac{\Gamma_{H\text{-}W} \Phi_H{}^+}{\rho_w} \qquad [5]$$

where ρ_w denotes the volume particle density of tungsten. This motion of the surface causes implanted hydrogen to be liberated. A second important process is the diffusion of hydrogen in the converter material. These two processes lead to the following diffusion equation,

$$\frac{\partial c(z,t)}{\partial t} = - D \frac{\partial^2 c(z,t)}{\partial z^2} - v_{sput} \frac{\partial c(z,t)}{\partial z} + \frac{\alpha \Phi_{H^+}}{c_{sat} d \sqrt{\pi}} \exp - \left(\frac{z - r}{d}\right)^2$$

$$\text{i) } c(z,0)=0 \qquad \text{ii) } c(\infty,t)=0 \qquad \text{iii) } D\frac{\partial c(z,t)}{\partial z} = \frac{\alpha \Phi_{H^+} - \Phi_{H^*} - \Phi_{des}}{c_{sat}} \qquad [6]$$

where we assumed a Gaussian implantation profile. c(z,t) denotes the relative concentration of hydrogen, as a function of the distance to the surface and time, i.e. $c(z,t)=c_H(z,t)/c_{sat}$. D is the diffusion coefficient for implanted particles in the tungsten bulk; r and d are the range and deviation of the implantation profile respectively and α is the implanted fraction. The third (iii) boundary equation for the stationary state reduces to $\Phi_{H^*} = \alpha\Phi_{H^+} - \Phi_{des}$. As explained in Ref. 20, there is a relation between sputtering and desorption of hydrogen from the surface, depending on the incoming flux of protons. For higher incoming flux the stationary branching ratio of sputtered relative to desorbed hydrogen shifts towards sputtering, i.e. the total number of sputtered hydrogen atoms increases more than linearly with the incoming flux, until a saturation level is reached.

III. CESIUM COVERAGE OF A TUNGSTEN SURFACE IMMERSED IN A CESIUM SEEDED HYDROGEN DISCHARGE

The converter surface is exposed to a flux of positive cesium ions and hydrogen ions. Calculations of the mean free path for ionization of thermal cesium atoms in a hydrogen plasma indicate that with a vapor injection scheme all cesium atoms are ionized before they reach the converter surface. Therefore in the model only cesium ions and hydrogen ions are used as the incoming fluxes. The corresponding fluxes are denoted as Φ_{Cs} and Φ_H, respectively. For simplicity, the presence of molecular ions (i.e. H_2^+ or H_3^+ ions) is neglected. A fraction of all incident cesium particles is trapped at the surface, a fraction is implanted in the tungsten and the remaining fraction is scattered. Furthermore, adsorbed particles are sputtered by incident cesium ions and protons, which have been accelerated by the negative converter

potential. Thus sputtering and reflection contribute to a flux of cesium particles leaving the surface. Note, that desorption of cesium from the surface in the temperature range we are using (< 200 °C) is negligible. The cesium particles leaving the surface are either neutral or positively charged. The ion component returns to the surface due to the electric field in the plasma sheath. The neutral component flows to the plasma. Note that it is implicitly assumed here that the mean free path for ionization is larger than the sheath thickness. The returning ions initiate a new step of trapping, scattering and sputtering. Consequently, a loop structure in the adsorption process develops. The resulting cesium coverage at the surface of the converter can be calculated as is outlined in appendix I.

The incoming positive ions reach the converter with an energy E_i, which is proportional to the converter potential V_c minus the plasma potential V_p, $E_i = e\,|V_c - V_p|$ electronvolt. In Fig. 2 the calculated cesium coverage is shown as a function of the converter potential for various implantation fractions α, of cesium. The cesium ion contribution to the total ion current on the converter, $\Phi_{Cs}/(\Phi_{Cs}+\Phi_H)$, is taken equal to 1 %. For α = 100 % the curve agrees with the measurements of Tompa et al. For α = 0 the curve coincides with the calculations of van Amersfoort et al. TRIM calculations yielded a constant implantation fraction of around 80 % for the energy range 30-300 eV. Using the known relation between cesium coverage and work function we can deduce that a minimum in the work function occurs for a converter potential of the order of -130 V for an implantation fraction of 80 %. Van Wunnik showed that a lower work function results in a higher H^- ion yield.[20] The existence of a maximum in the extracted H^- current as a function of the converter potential has been observed in various sources employing cesium vapor injection.[3,4] In Fig. 3, the coverage is plotted versus the cesium fraction in the discharge for a typical converter potential of -150 V for an implantation fraction of 80 % and 30 %. For low seeding fractions we see an increase of the coverage with increasing fractions and for higher fractions the coverage saturates. From this figure we may conclude that it is not useful to "overdose" the discharge

with cesium to obtain a higher coverage, as is consistent with experimental observation obtained at the Lawrence Berkeley Laboratory.[22]

In view of the considerations and calculations given above, a cesium coverage independent of the converter potential cannot be obtained using a cesium vapor deposition method. From the calculations it is clear that the only method of increasing the coverage is to increase the flux of neutral cesium atoms towards the surface. The method we choose to increase this flux is to use liquid cesium diffusing through a porous converter.

IV EXPERIMENT

The set-up of the experiment is shown in Fig. 4, the system is discussed in great detail in Ref. 23. In summary, the plasma is produced with a hollow cathode arc discharge. The plasma is confined by an axial magnetic field of 200 Gauss. It is bent in a U-shape to avoid contamination of the converter with cathode material. The source contains two cathodes, however the experiments are done using only a single one. The arc current can be varied from 5 to 35 A. The converter potential can be biased from 0 to -350 V with respect to the anode potential. The formed negative ions are collected in a Faraday cup after removal of free electrons by means of a magnetic field. Furthermore, the Faraday cup can be replaced by a magnetic analyzer with which the mass and energy distribution of the "self-extracted" negative ion beam can be measured.

The converter is made from sintered tungsten with a porosity of 20%. Behind the porous tungsten plate is a reservoir with liquid cesium which can diffuse through the plate. The reservoir can be pressurized with argon gas. In a small test setup we confirmed that with this configuration a flow of the order of 10^{18} atoms cm^{-2} s^{-1} is obtainable at a tempertaure of around 100° C. The latter is more than three orders higher than the rate with which cesium is removed from the surface via sputtering. Operating this converter showed that it was no longer necessary to pressurize the reservoir once the porous tungsten was saturated with cesium. Apparently, the concentration gradients at the surface are sufficiently large to

replenish all cesium which is removed via sputtering. Even after seeding the discharge with heavy ions like xenon or argon, no depletion of the surface coverage was observed.

IV.a Experimental Results

The mass distribution as obtained with a magnetic analyzer, described in detail in Ref.13, confirmed that the negative ion beam contained only H^- ions. The position of the peak in the energy distribution as a function of the potential difference between converter and detector is shown in Fig. 5. The straight line denotes the energy expected for particles produced via sputtering. The uncertainty in the position of the peak is of the order of 20 %. For a converter potential greater than 200 V the energy distribution peak follows the straight line indicating that the production mechanism is fully dominated by sputtering. Below 200 V there is a contribution of directly recoiling hydrogen atoms. Measurements of the conversion efficiency (i.e. the ratio of the extracted negative ion current and the positive ion current incident on the converter surface) as earlier reported by van Os, Granneman and van Amersfoort,[23] show an increase at low converter potentials and a saturation at higher potentials.

No clear dependence was observed as a function of the arc current, i.e. the positive ion current density on the converter surface. The values obtained for the conversion efficiency are an order of magnitude lower than values obtained with cesium seeded discharges, see e.g. Ref. 20. Furthermore, no clear optimum is observed as a function of the converter potential, whereas in the other sources an optimum for V_c between -100 and -200 V is reported. The latter is probably related to the scheme we used to obtain a surface coverage of cesium. This coverage is independent of the discharge characteristics and the converter bias, whereas, the aforementioned maximum in conversion efficiency was observed in sources using a cesium vapor deposition method. In section III. we showed that with such a method the cesium coverage (i.e. the work function of the converter surface) is a function of the converter bias which accounts for the observed maximum.

The conversion efficiency showed no dependence on arc current, i.e. incoming flux. We showed in a previous report[13] that in the case of a diffusion limited process, a barium converter, the conversion efficiency increases with increasing incoming flux. The diffusion coefficient for hydrogen in barium is 3. 10^{-9} m^2 s^{-1} at T=470 K [24], whereas for hydrogen in tungsten it is 10^{-15} m^2 s^{-1} [25]. It is safe to assume that the diffusion coefficient for hydrogen in liquid cesium is very large compared to diffusion of hydrogen in tungsten or barium. We may therefore conclude that any build up of a hydrogen concentration should be due to the accumulation of hydrogen in the tungsten grains of the sintered converter. A calculation of the actual hydrogen concentration in the tungsten grains close to the surface can be found in Appendix II. The conclusion here is that the tungsten grains become rapidly saturated with hydrogen. This forms a steady supply of hydrogen towards the surface layers.

At the surface the hydrogen is sandwiched between the cesium monolayer[26] and the tungsten surface, therefore we cannot simply take the sputter coefficient for incident hydrogen ions on adsorbed hydrogen in order to calculate the flux of hydrogen atoms leaving the surface. Instead, we propose to utilize the sputter coefficient for incident particles on cesium. In other words, it is assumed that the removal of cesium atoms from the surface results in the liberation of hydrogen atoms. In this combined process of sputtering cesium which liberates hydrogen, we make the crucial assumption that *on the average one hydrogen atom is liberated for each cesium atom sputtered (e.g.* $\Gamma_{H\text{-}H} \approx 1$*).* Based on this assumption we can rewrite Eq. [4] using Eq. [2] as

$$\Phi_{H^-} = \eta_H \, \Gamma_{H\text{-}H} \, \Gamma_{H\text{-}Cs} \, \Phi_{H^+} \approx \eta_H \, \Gamma_{H\text{-}Cs} \, \Phi_{H^+} \qquad [7]$$

where η_H is the ionization probability. The sputter coefficient can be calculated as a function of the energy of the incident particles (i.e the converter potential) with the formulas of Bohdansky.[27] Fig. 6 shows the conversion efficiency as a function of the sputter coefficient

for hydrogen on a full monolayer of cesium adsorbed on tungsten. From a least square fit of the curve in Fig. 6 we found an attachment probability, $\eta_H = 0.10 \pm 0.03$, which is of the same order as attachment probabilities obtained by model calculations, see Fig. 1.

To further investigate the importance of the adlayer of cesium atoms "screening" the adsorbed hydrogen atoms, one could artificially enhance the sputter removal rate by admitting a heavy rare gas (Xe or Ar) to the discharge. Van Os and van Amersfoort[28] did such an experiment which showed an increase of an order of magnitude of the conversion efficiency with increasing heavy ion flux. The sputter coefficient for Ar^+ and Xe^+ incident on cesium/tungsten, is rougly two orders of magnitude larger compared to incident H^+. Fig.7 shows the dependence of the conversion efficiency on the total sputter coefficient , $\Gamma_{tot} = f_{rare}\ \Gamma_{rare\text{-}Cs} + f_H\ \Gamma_{H\text{-}Cs}$, where f_{rare} and f_H are the abundances of rare gas atoms and H^+ ions respectively, with $f_{rare}+f_H=1$. Assuming again that every sputtered cesium atom results in one sputtered hydrogen atom and plotting the conversion efficiency as a function of the sputter coefficient in a similar way as described above only using now the total sputter coefficient instead of the sputter coefficient of hydrogen on cesium we arrive at an attachment probability of $\eta_H = 0.09 \pm 0.02$, consistent with the earlier determined values.

V. COMPARISON OF BINARY (H-Ba) AND TERNARY (H-Cs/W) CONVERTER SCHEMES

As motivated in the previous sections, the negative ion yield from a surface conversion source is directly proportional to the attachment probability multiplied by the flux of sputtered hydrogen atoms. For a binary converter (e.g. barium) the following equation describes the dominant production process, see Ref. 20 and section II.a. Upon the assumption that the self sputtering coefficient for hydrogen on adsorbed hydrogen is close to unity, $\Gamma_{H\text{-}H} \approx 1$, this equation further reduces,

$$\Phi_H^- = \left(\eta_H^{Ba} \quad \frac{c_H}{c_{sat}} \Gamma_{H\text{-}H}\right)\Phi_H^+ \approx \left(\eta_H^{Ba} \quad \frac{c_H}{c_{sat}}\right)\Phi_H^+ \qquad [8]$$

For the ternary system (Cs/W) the equation which was arrived at in the previous section could easily have been derived from Eq. 8 by adding the "screening" factor $\Gamma_{H\text{-}Cs}$. In the previous section we showed that the sandwiched hydrogen layer is saturated, therfore $\frac{c_H}{c_{sat}} \approx 1$.

$$\Phi_H^- = \left(\eta_H^{Cs/W} \quad \frac{c_H}{c_{sat}} \Gamma_{H\text{-}H}\, \Gamma_{H\text{-}Cs}\right)\Phi_H^+ \approx \left(\eta_H^{Cs/W} \quad \Gamma_{H\text{-}Cs}\right)\Phi_H^+ \qquad [9]$$

Here η_H^{Ba} and $\eta_H^{Cs/W}$ denotes the attachment probability for barium or cesiated tungsten, respectively. Eq, 8 and 9 differ considerably in the following areas: i) The scaling of the negative ion yield with the incident positive ion current density on the converter and ii) the scaling of the negative ion yield with the density of heavy ions in the discharge. The justification of the classification into two classes of converters [the *binary* (H-Ba) and *ternary* (H-Cs/W) converter arrangement] will be obvious from the following experimentally observed scalings in the two areas described above:

The first observation is outlined in Fig. 8 where the conversion efficiency, η_H, for a barium- and a cesiated-tungsten converter is shown as a function of the incident positive ion current density. The conversion efficiency for Cs/W is constant with positive-ion current density. The hydrogen concentration is sandwiched between the cesium adlayer and the tungsten substrate. Therefore, no increase is expected as shown in section IV. For barium the conversion efficiency increases with increasing positive-ion current density. This has been explained by (and confirmed by model calculations of) an increase of the hydrogen concentration in the barium surface layers with increasing ion flux.

Fig. 9 shows the measured conversion efficiency for a barium and a Cs/W converter as a function of the partial pressure of argon and xenon. For the cesium converter, a sharp

increase is observed, when the partial pressure reaches 0.01 Pa. This is explained by an increase in the sputter yield of hydrogen atoms (section IV.a) because sufficient hydrogen is available for sputtering. For barium a sharp decrease is observed when the partial pressure rises. This is explained by a decrease of the hydrogen concentration in the barium surface layers by the enhanced sputtering by heavy ions.

VI. CONCLUSIONS

Model calculations of the cesium household for a solid converter immersed in a cesium seeded discharge show that the cesium coverage of the converter is a strong function of the converter bias. The set-up we used, a porous tungsten converter with liquid cesium diffusing through it, always has a full monolayer coverage of cesium due to the efficient replenishing of the sputtered cesium. Moreover, this arrangement results in a low cesium content of the hydrogen discharge which enabled us to study the effect of heavy ion sputtering in the negative ion production mechanism.

Model calculations on the hydrogen household of this converter show that the surface layers are saturated with hydrogen due to the very low diffusion coefficient of hydrogen in tungsten. The hydrogen located near the surface can only be liberated via removal of cesium from the surface by means of sputtering since the hydrogen is sandwiched between the cesium adlayer and the tungsten. In this case we call the negative ion formation process sputter limited. This is in contrast with experiments done with a solid barium converter, due to the high diffusion coefficient for hydrogen in barium no saturation occurs, this regime is diffusion limited. In the latter case, the conversion efficiency is an almost linear function of the incident positive hydrogen ion flux on the surface, whereas for a cesium/tungsten converter no such increase is observed. This led us to categorize surface conversion sources into two groups: i) binary system (like H-Ba) where the adsorbed hydrogen in the surface layers is directly

sputtered by the incoming ions, and ii) ternary system (like H-Cs/W) where the adsorbed hydrogen in the surface layers is indirectly released via the sputter removal of adlayer atoms.

ACKNOWLEDGEMENTS

The authors gratefully acknowledge H.J. Timmer for his technical assistance during the experiments and R.M.A. Heeren for his help in the calculations of the cesium coverage, at the FOM Institute in Amsterdam. This work is part of the research program of the association agreement between the Stichting voor Fundamenteel Onderzoek der Materie (FOM) and EURATOM, and was made possible by financial support from the Nederlandse Organisatie voor Wetenschappelijk Onderzoek (NWO) and EURATOM. This work has also been supported, in part, by the Director, Office of Energy Research, Office of Fusion Energy of the U.S. Department of Energy under Contract No. DE-AC03-76SF00098.

Appendix I

The evolution of the cesium coverage is calculated as follows. The surface is exposed to the involved fluxes for an incremental time of dt seconds and the loop structure initiated by this incremental exposure. A rate equation is obtained from a balance of source and sink terms. The equilibrium coverage due to adsorption can be found by determining the time independent solution of this rate equation. Van Amersfoort et. al found for the coverage, θ_{Cs} (in monolayers) due to adsorption; [29]

$$\theta_{Cs,a}=\frac{(1-\alpha)\{P(E_i,\theta_{Cs})+\eta_{Cs}(\theta_{Cs})[1-P(E_i,\theta_{Cs})]\}\,\Phi_{Cs}}{\{1-\eta_{Cs}(\theta_{Cs})\}\{\Gamma_{Cs\text{-}Cs}(E_i,\theta_{Cs})\Phi_{Cs}+\Gamma_{H\text{-}Cs}(E_i,\theta_{Cs})\Phi_H\}} \qquad [A.I.1]$$

where α is the implanted fraction, E_i is the incident energy, $P(E_i,\theta_{Cs})$ is the trapping probability for cesium ions and $\eta_{Cs}(\theta_{Cs})$ is the ionization degree of the sputtered cesium particles as a function of the surface coverage. $\Gamma_{Cs\text{-}Cs}(E_i,\theta_{Cs})$ and $\Gamma_{H\text{-}Cs}(E_i,\theta_{Cs})$ are the sputter coefficients, respectively for incident cesium and hydrogen ions on an adsorbed cesium layer on tungsten.

So far we did not discuss the consequences of the cesium ions that are implanted into the tungsten surface. Tompa, Carr and Seidl set up a model to calculate the equilibrium coverage due to implantation.[30] Their model is based upon a differential equation analogous to Eq. [6]. The only difference is that they accounted for the effect that implanted cesium particles in the tungsten bulk result in a rearrangement of the tungsten. For hydrogen as incident particles, this effect can be neglected. In their model we defined the incoming flux as $\Phi_{in} = \Phi_H + \Phi_{Cs}$. For the determination of the cesium coverage, only the sputtering of the target material by hydrogen ions is relevant, implantation of hydrogen into the tungsten surface is not described. If diffusion is neglected, the result of this model is the following analytical expression

$$\theta_{Cs,i} = \frac{\kappa\ \alpha}{(\Gamma_{Cs\text{-}W}(E_i) + \beta\Gamma_{H\text{-}W}(E_i))} \qquad [A.I.2]$$

where κ can be calculated from the measurements of Tompa et al. and $\Gamma_{Cs\text{-}W}(E_i)$ and $\Gamma_{H\text{-}W}(E_i)$ are the sputter coefficients for incident cesium and hydrogen ions on tungsten, respectively.[31] The factor β is defined by $\Phi_H = \beta\ \Phi_{Cs}$. This gives an additional source term in the rate equation as formulated by van Amersfoort et al.[29]. The steady-state solution of the rate equation can be written as the following implicit equation,

$$\theta_{Cs} = \frac{(1-\alpha)\{P(E_i,\theta_{Cs}) + \eta_{Cs}(\theta_{Cs})[1-P(E_i,\theta_{Cs})]\}\ \Phi_{Cs}}{\{1-\eta_{Cs}(\theta_{Cs})\}\{\Gamma_{Cs\text{-}Cs}(E_i,\theta_{Cs})\Phi_{Cs} + \Gamma_{H\text{-}Cs}(E_i,\theta_{Cs})\Phi_H\}} + \frac{\kappa\ \alpha}{(\Gamma_{Cs\text{-}W}(E_i) + \beta\Gamma_{H\text{-}W}(E_i))}. \qquad [A.I.3]$$

The implantation fraction α determines which of the two processes, adsorption or implantation, is dominant.

Appendix II

In order to calculate the hydrogen concentration in the tungsten grains we idealized the sintered converter as made up from a stack of tungsten cylinders with varying diameters, with typical dimensions of the order of 10 μm, immersed in liquid cesium. Only the front surface of the cylinder is exposed to the incoming flux of hydrogen ions. Due to diffusion of hydrogen in the tungsten cylinder (grain) it will eventually arrive at the boundary of the cylinder. At this point the hydrogen can either dissolve into the liquid cesium or diffuse along the cesium tungsten interface. Both processes are believed to be much faster than the diffusion process inside the tungsten, which means that we have an efficient removal of hydrogen at the cylinder surface. Therefore, we assume that at the boundary of the cylinder the concentration of hydrogen is close to zero. For this cylinder we have to solve Eq. [6]. The ratio of these differntentials on the right hand side in Eq. [6] can de expressed as

$$\kappa = \frac{D}{v_{sput}\ w} \qquad \text{[A.II.1]}$$

where w is a typical dimension in the process, e.g. the implantation depth. Substitution of numerical values gives a value for κ of the order of 400 which means that we can neglect the motion of the surface in Eq. [6]. Furthermore, we assume that the incident flux of hydrogen is implanted directly at the surface, i.e., as a delta function rather than providing a gaussian implantation profile.

This gives us the following differential equation in cylindrical coordinates for one of the tungsten cylinders with radius a;

$$\frac{1}{D}\frac{\partial c(z,r,t)}{\partial t} = \frac{\partial^2 c(z,r,t)}{\partial r^2} + \frac{1}{r}\frac{\partial c(z,r,t)}{\partial r} + \frac{\partial^2 c(z,r,t)}{\partial z^2} \qquad 0 \le r < a, \quad z > 0,$$

$$\text{for: } r = a\ ,\ c(z,r,t) = 0 \quad \text{and} \quad \text{for: } z = 0,\ -D\frac{\partial c(z,r,t)}{\partial z} = \frac{\alpha\ \Phi_{H^+}}{c_{sat}} \qquad \text{[A.II.2]}$$

where z is the position along the cylinder, r is the radial coordinate of the cylinder, D the diffusion coefficient of hydrogen in tungsten, α the implantation fraction and Φ_{H^+} the incident flux of hydrogen ions. The time independent solution of Eq. [A.II.2] can be derived from an analytical solution of an analogous heat diffusion problem by Carslaw and Jaeger.[32] They found for a semi-infinite cylinder with zero concentration at r = a and in which the front surface has a concentration defined by $c(o,r) \equiv f(r)$:

$$c(z,r) = \frac{2}{a^2} \sum_{n=1}^{\infty} \frac{J_0(r\alpha_n)}{J_1(r\alpha_n)} \exp(-\alpha_n z) \int_0^a r\, f(r)\, J_0(r\alpha_n)\, dr \ , \qquad \text{[A.II.3]}$$

where α_n are the positive roots of $J_0(a\alpha_n) = 0$ and J_i represents the i-th order Bessel function. In our calculations we took f(r) = c (constant) and calculated $D\partial c/\partial z|_{z=0}$ to match the incoming flux of positive hydrogen ions according to the second boundary condition in Eq. [A.II.2]. For an incident hydrogen ion flux of 20 mA/cm^2 ($\approx 10^{17}$/cm^2 s) a hydrogen concentration is obtained of the order of the number density of tungsten, which becomes larger for larger grain diameters. Hence, we conclude that in the case of a sintered tungsten converter filled with liquid cesium, the tungsten surface layers are always saturated with hydrogen.

FIGURE CAPTIONS

Fig. 1 The attachment probability as a function of the energy with which the hydrogen atom leaves normal to the surface. The heavy solid curve is for half a monolayer of cesium on tungsten, the dashed line is for a cesium surface and the fine solid line for a barium surface.

Fig. 2 The calculated cesium coverage of the converter surface as a function of the converter potential for various implantation fractions.

Fig. 3 The calculated cesium coverage of the converter surface as a function of different cesium seeding fractions for a converter potential of -150 V and for implantation fractions of 30 and 80 %.

Fig. 4 Experimental arrangement of the Amsterdam Light Ion Conversion Experiment (ALICE).

Fig. 5 The measured position of the peak in the energy distribution vs the potential difference between converter and detector.

Fig. 6 The conversion efficiency as a function of the sputter coefficient for hydrogen on adsorbed cesium.

Fig. 7 The conversion efficiency as a function of the total sputter coefficient for a xenon or argon seeded hydrogen discharge.

Fig. 8 The conversion efficiency as a function of the incident positive-ion current density for a barium and a cesiated tungsten converter. Converter potential is -250 V. No pressure is applied to the cesium reservoir. Lines are shown to guide the eye.

Fig. 9 The conversion effeciency as a function of the partial gas pressure of a rare gas additive for a barium and a cesiated tungsten converter. Converter potential is -200 V. No pressure is applied to the cesium reservoir. Lines are shown to guide the eye.

REFERENCES

1 K.H. Berkner, R.V. Pyle and J.W. Stearns, Nucl. Fusion **15** (1975) 249.

2 Yu.I. Belchenko, G.I. Dimov and V.G. Dudnikov, Nucl. Fusion **14** (1974) 113.

3 E.J. Britt, J.L. Desplat, M. Korringa and K.N. Leung, J. Vac. Sci. Technol. **A 3** (1985) 1241.

4 A.I. Hershcovitch, V.J. Kovarik and K. Prelec, Rev. Sci. Instrum. **57** (1986) 827.

5 J. Kwan, G.D. Ackerman, O.A. Anderson, C.F. Chan, W.S. Cooper, G.J. deVries, A.F. Lietzke, L. Soroka and W.F. Steele, Rev. Sci. Instrum. **57** (1986) 831.

6 B. Piosczyk and G. Dammertz, Rev. Sci. Instrum. **57** (1986) 840.

7 J.L. Desplat and C.A. Papageorgopoulos, Surf. Sci. **92** (1980) 97.

8 K.N. Leung and K.W. Ehlers, Rev. Sci. Instrum. **53** (1982) 803.

9 P.J.M. van Bommel, K.N. Leung and K.W. Ehlers, J. Appl. Phys. **56** (1984) 751.

10 Yu.I. Belchenko and A.S. Kupriyanov, Revue Phys. Appl. **23** (1988) 1885.

11 M. Wada, R.V. Pyle and J.W. Stearns, *Proc. of the 3rd Int. Symp. on Production and Neutralization of Negative Ions and Beams*, Upton, NY, 1983, AIP Conf. Proc. 111, p247.

12 K.N. Leung and K.W. Ehlers, J. Appl. Phys. **52** (1981) 3902.

13 C.F.A. van Os, P.W. van Amersfoort and J. Los, J. Appl. Phys. **64** (1988) 3863.

14 J.P. Biersack and W. Eckstein, Appl. Phys. (Berlin) **A 34** (1984) 73.

15 M.S. Huq, L.D. Doverspike and R.L. Champion, Phys. Rev. **A 27** (1983) 2831.

16 J.S. Risley and R. Geballe, Phys. Rev. **A 9** (1974) 2485.

17 J. R. Hiskes, J. de Physique 40, Colloque C7 Vol. 2, p. C7-179 (1979). See also J. R. Hiskes and A. Karo, Procs. of the Symp. on Production and Neutralization of Negative Hydrogen Ions and Beams, Brookhaven, BNL 50727 (1977) p. 42.

18 R. Gomer and L. W. Swanson, J. Chem. Phys. **38** (1963) 1613.

19 J.J.C. Geerlings, P.W. van Amersfoort, L.F.Tz. Kwakman, E.H.A. Granneman, J. Los and J.P. Gauyacq, Surf. Sci. **157** (1985) 151.

20 J.N.M. van Wunnik, J.J.C. Geerlings, E.H.A. Granneman and J. Los, Surf. Sci. **131** (1983) 17.

21 P.W. van Amersfoort, J.J.C. Geerlings, R. Rodink, E.H.A. Granneman and J. Los, J. Appl. Phys. **59** (1986) 241.

22 A.F. Lietzke, private communication.

23 C.F.A. van Os, E.H.A. Granneman and P.W. van Amersfoort, J. Appl. Phys. **61** (1987) 5000.

24 D.T. Peterson and C.C. Hammerberg, J. Less-Common Metals **16** (1968) 457.

25 A. P. Zakharov et al, Diffusion and Defect Data **9** (1974) 244.

26 C.A. Papageorgopoulos and J.M. Chen, Surf. Sci. **39** (1973) 283.

27 J. Bohdansky, Nucl. Instr.&Meth. in Phys. Res. **B2** (1984) 587.

28 C.F.A. van Os and P.W. van Amersfoort, Appl. Phys. Lett. **50** (1987) 662.

29 P.W. van Amersfoort, Ying Chun Tong and E.H.A. Granneman, J. Appl. Phys. **58** (1985) 2317.

30 C.S. Tompa, W.E. Carr and M. Seidl, Appl. Phys. Lett. **48** (1986) 1048.

31 C.S. Tompa, W.E. Carr and M. Seidl, Appl. Phys. Lett. **49** (1986) 1511.

32 H.S. Carslaw and J.C. Jaeger, *Conduction of heat in solids*, Oxford university Press, 1959.

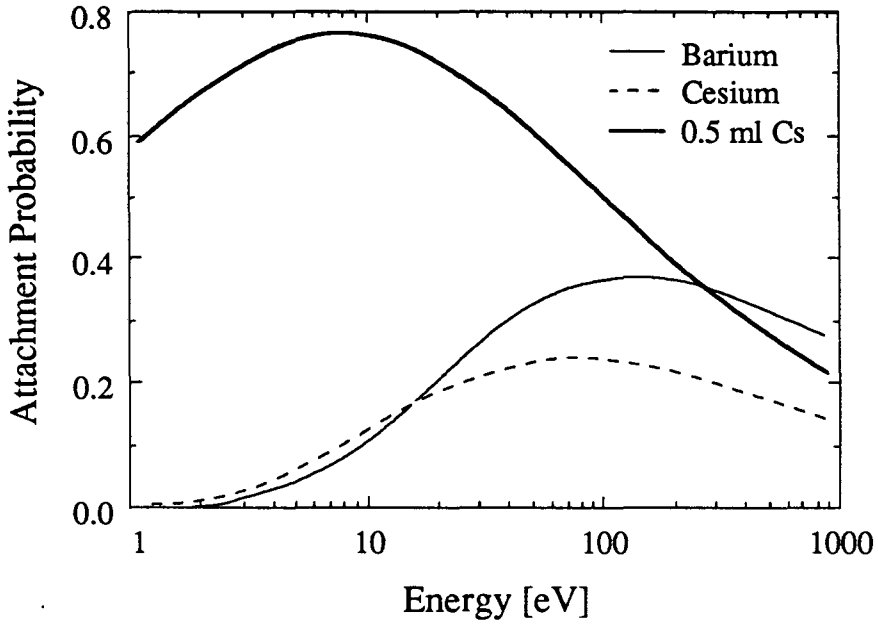

XBL 913-388

Fig 1.

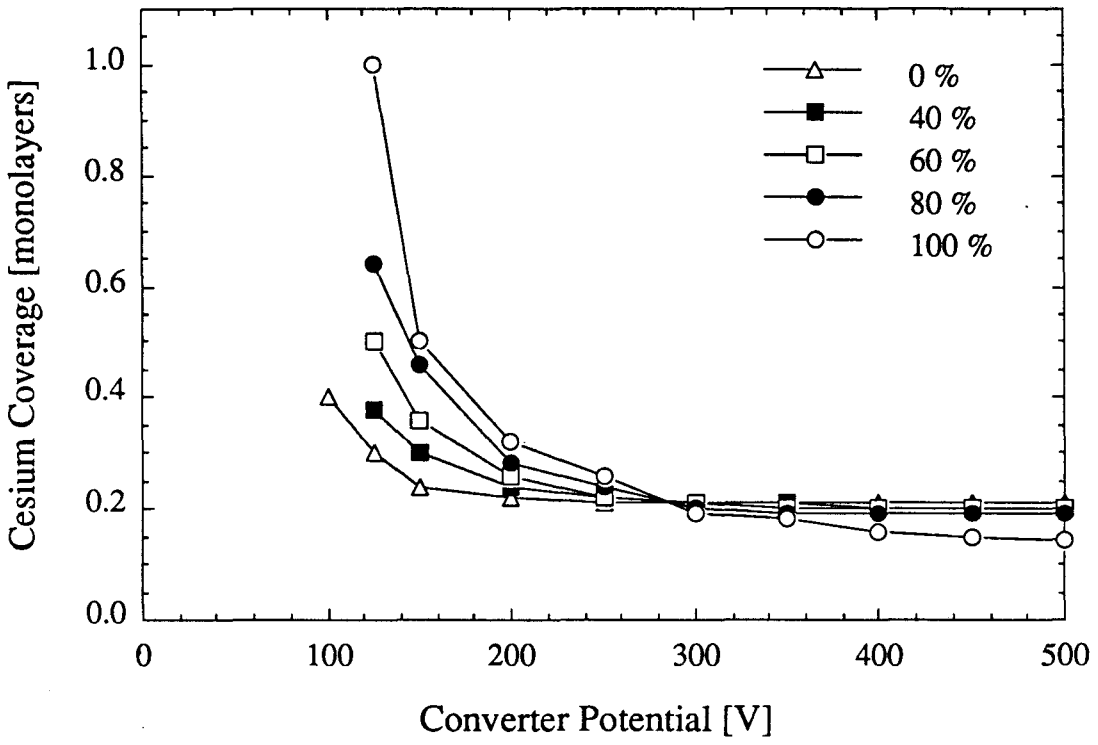

XBL 913-389

Fig. 2

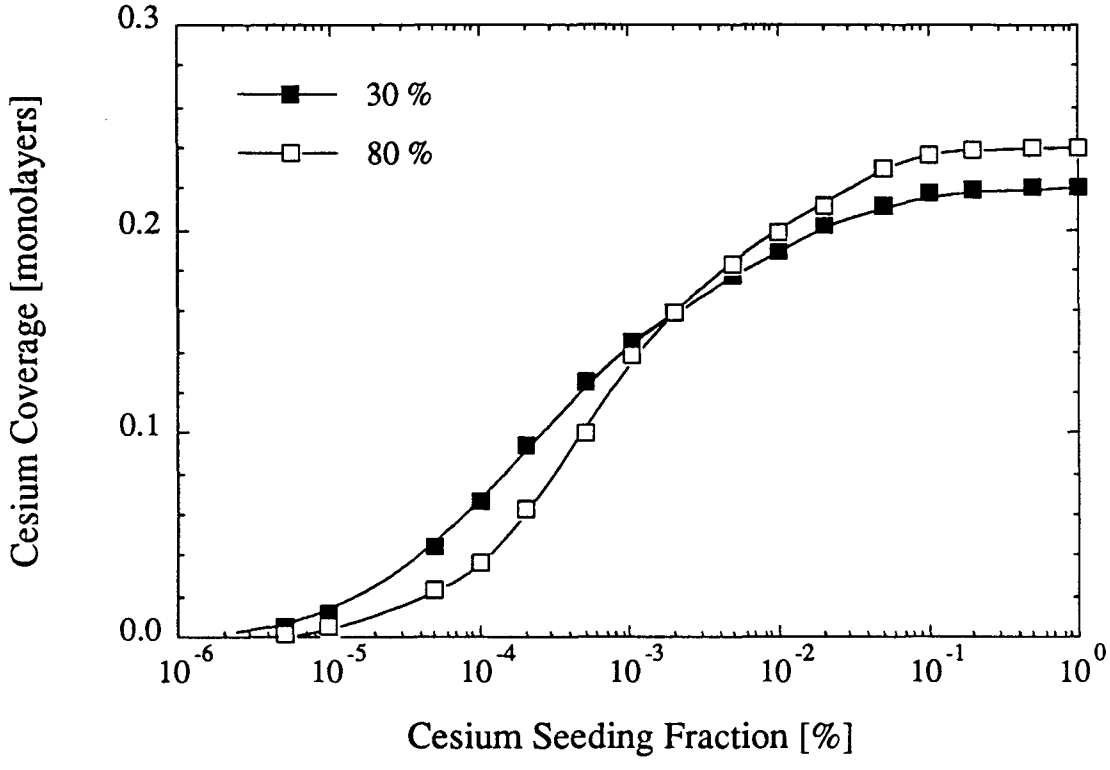

XBL 913-390

Fig. 3

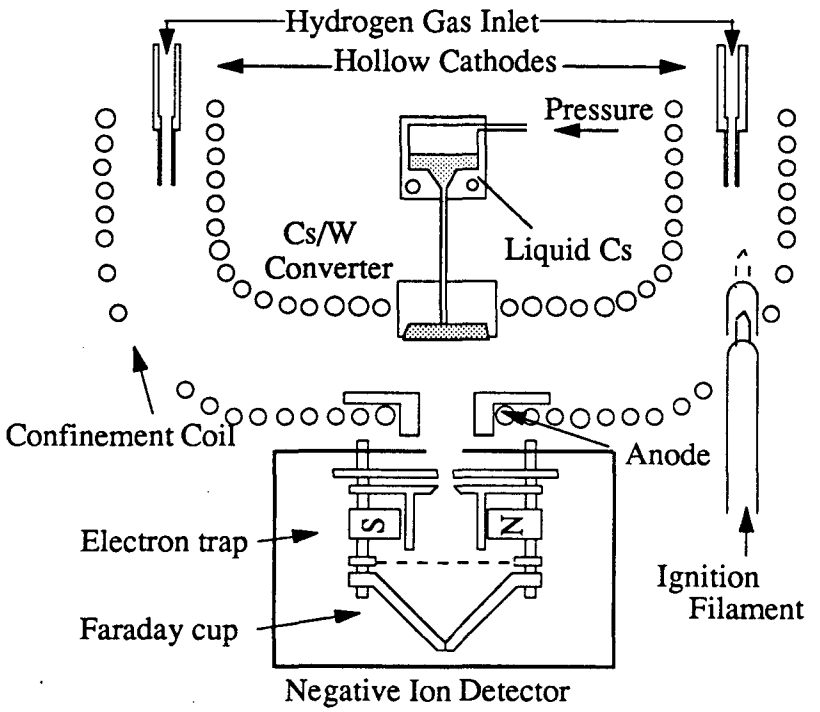

XBL 913-391

Fig 4

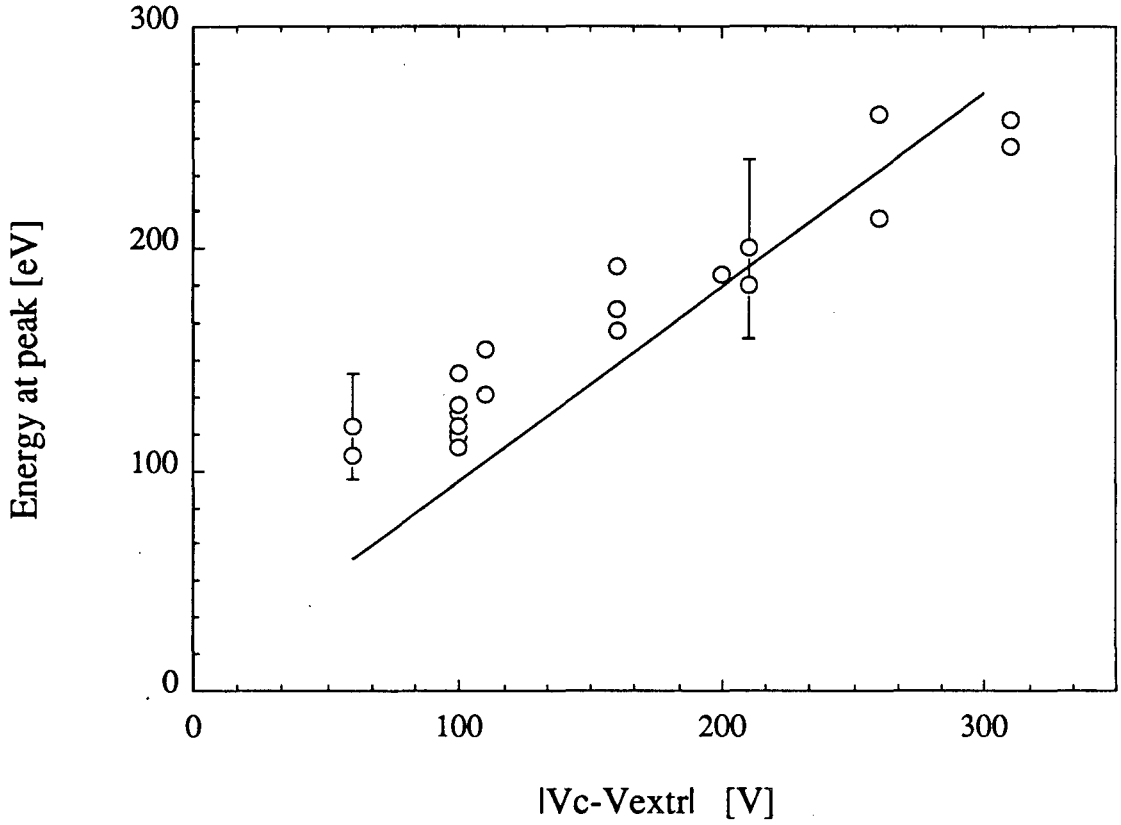

XBL 913-392

Fig. 5

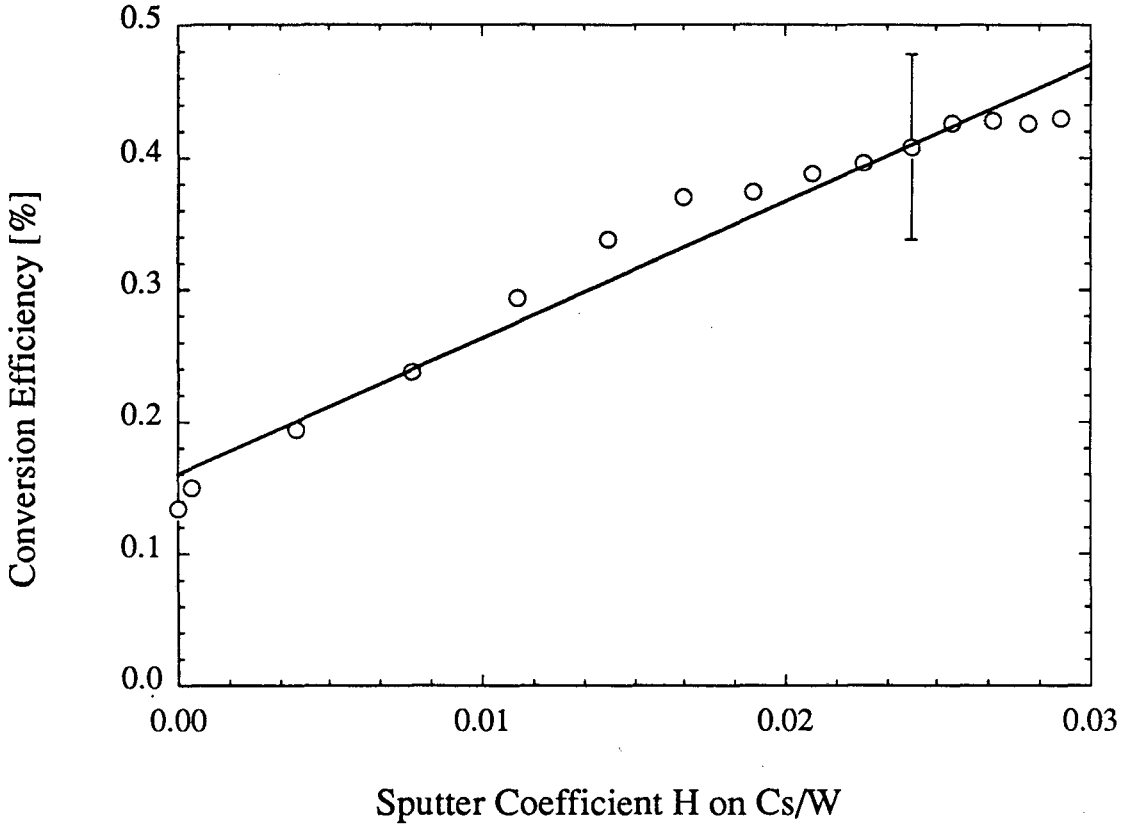

XBL 913-393

Fig. 6

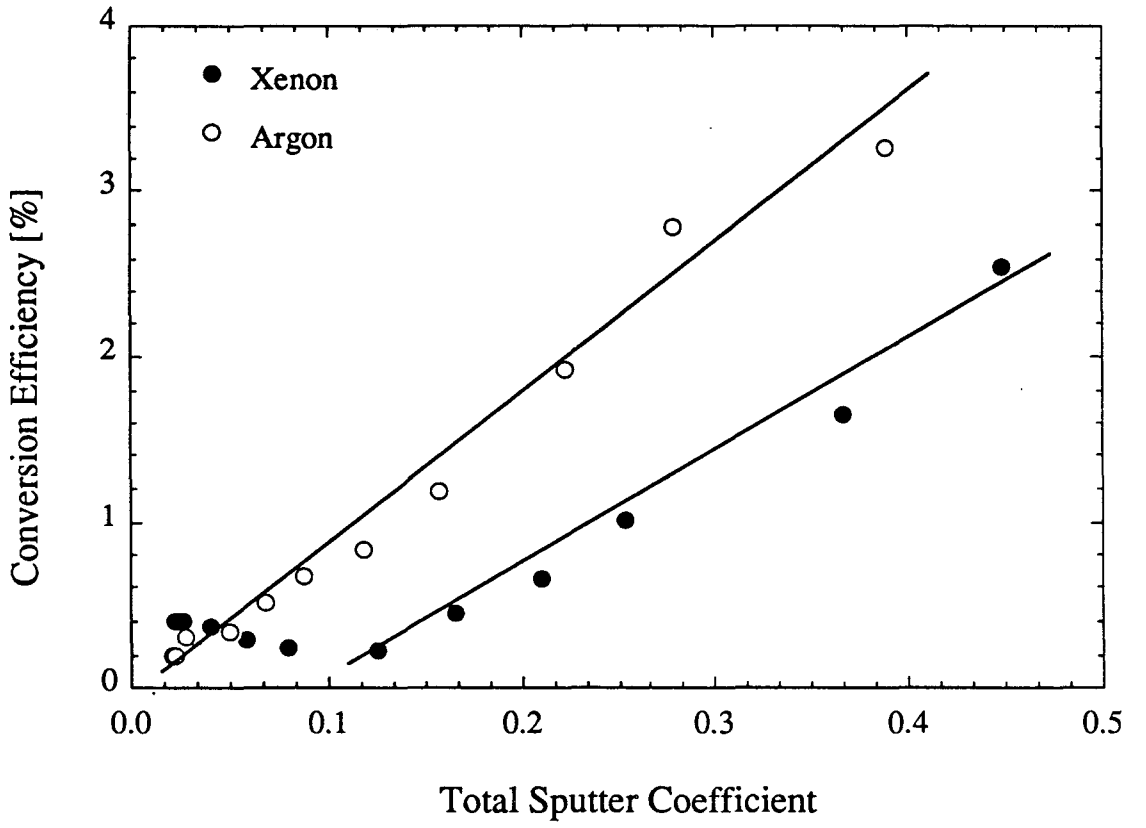

XBL 913-394

Fig. 7

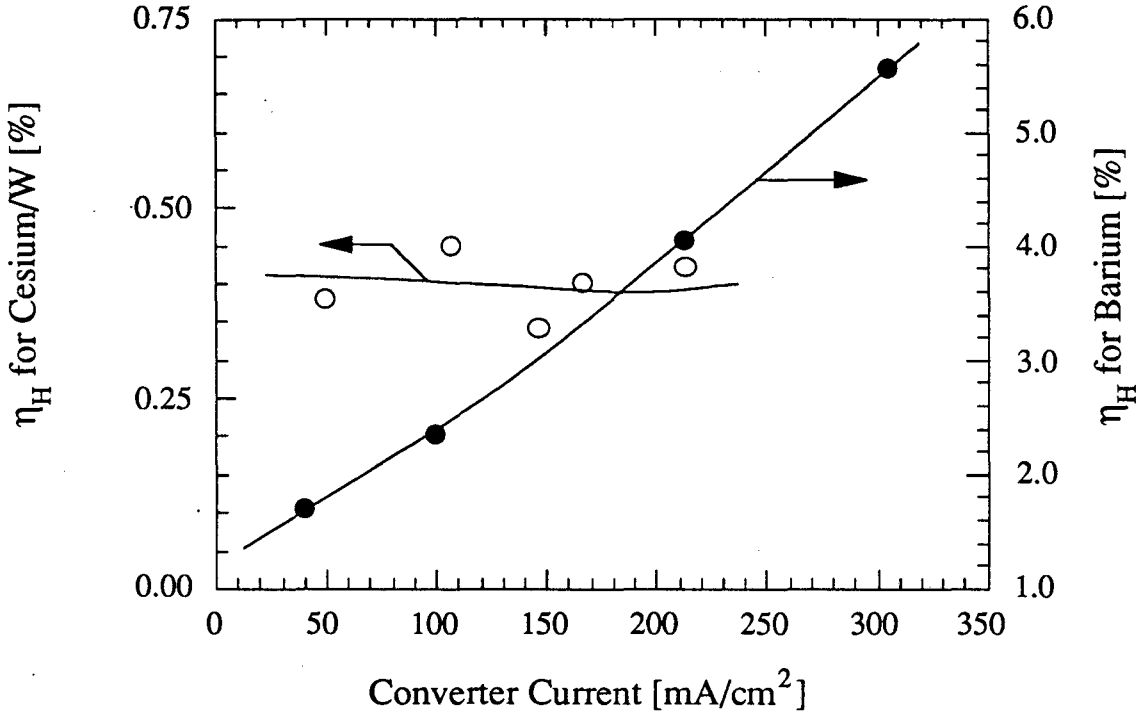

XBL 913-395

Fig. 8

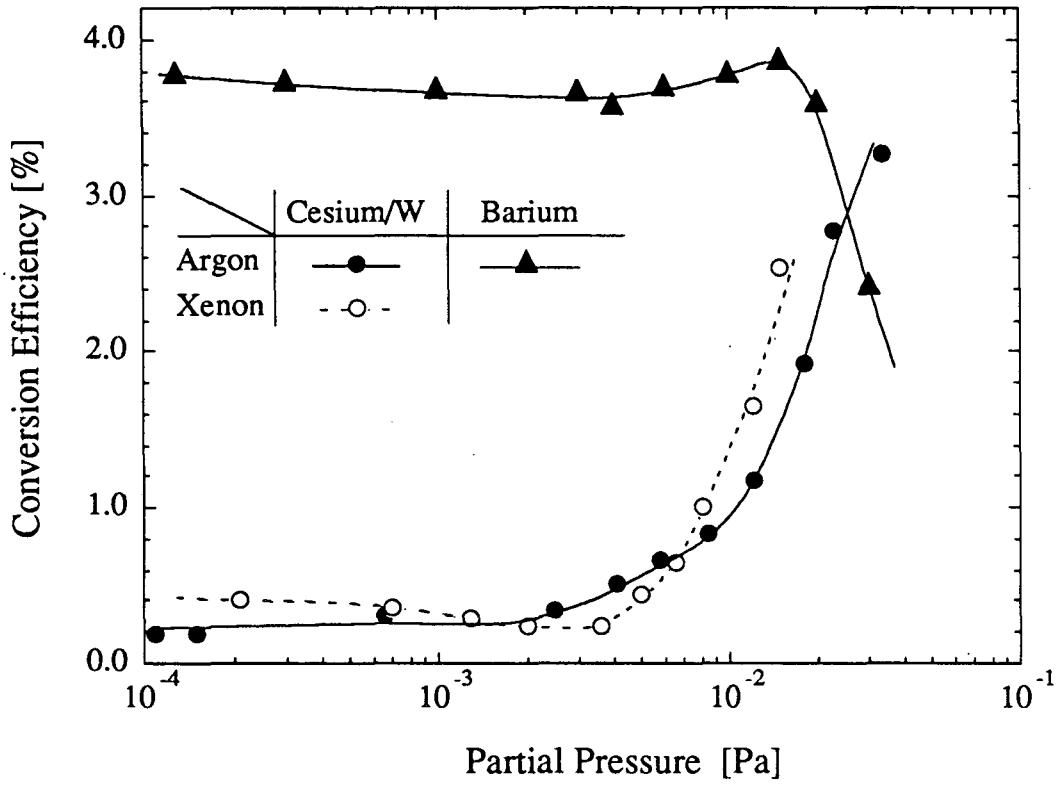

XBL 913-396

Fig. 9

LAWRENCE BERKELEY LABORATORY
UNIVERSITY OF CALIFORNIA
INFORMATION RESOURCES DEPARTMENT
BERKELEY, CALIFORNIA 94720